

## Entanglement in Anderson Nanoclusters

Peter Samuelsson and Claudio Verdozzi

Solid State Theory, Lund University, Solvegatan 14 A, 223 62 Lund, Sweden

(Dated: April 15, 2024)

We investigate the two-particle spin entanglement in magnetic nanoclusters described by the periodic Anderson model. An entanglement phase diagram is obtained, providing a novel perspective on a central property of magnetic nanoclusters, namely the temperature dependent competition between local Kondo screening and nonlocal Ruderman-Kittel-Kasuya-Yoshida spin ordering. We find that multiparticle entangled states are present for finite magnetic field as well as in the mixed valence regime and away from half filling. Our results emphasize the role of charge fluctuations.

PACS numbers: 3.67.Mn, 71.10.Fd, 03.67.-a, 75.75.+a

In the last decade, solid state systems have emerged as a promising stage for quantum information processing, due to the prospect of scalability and integrability with conventional electronics. A successful realization of solid state quantum information processing requires a detailed control of the quantum mechanical properties of the system. In this respect, a key property is entanglement, or quantum mechanical correlations, between the individual quantum bits; entanglement plays the role of basic resource for a large number of quantum information schemes [1]. In nanoscale solid state systems, internal degrees of freedom of individual electrons, like spin or orbital states, are natural candidates for quantum bits. This offers considerable scope for studies of electronic entanglement in nanosystems.

For spin entanglement, of particular interest are nanoclusters with magnetic impurities, realized experimentally e.g. by magnetic atoms on a surface [2], on a nanotube [3] or by coupled quantum dots [4]. Such nanoclusters display intriguing spin properties as the Kondo effect and antiferromagnetism, similar to what occurs in extended systems with dense magnetic impurities. For extended systems a central feature, described by the Doniach phase diagram [5], is the competition between formation of local Kondo spin singlets and a nonlocal Ruderman-Kittel-Kasuya-Yoshida (RKKY) spin ordering. A model which captures such behavior is the periodic Anderson model, PAM, a lattice of localized levels (with strong local repulsion) which hybridize with a conduction band. The PAM has been investigated intensively during the last decades [6] in connection with heavy fermion physics, non-fermi liquid behavior, etc [7].

To date, no studies are however available for entanglement in the PAM, only the related single [8] and two [9] impurity Anderson models and the simplified Kondo necklace model [10] have been considered. There are also investigations of entanglement in various spin cluster models [11, 12]. None of these models do however correctly capture the interplay of spin correlations and charge dynamics, characteristic of the PAM [6]. Only very recently the interest turned to systems where charge dynamics is important [13, 14]. These investigations show

ever only concerned the Hubbard model, focusing on entanglement in extended systems, at quantum phase transitions [15]. An investigation of the entanglement in nanoclusters described by the PAM is thus highly desirable.

In this work we perform such an investigation. Using exact diagonalization methods, ED, we study two-particle spin entanglement in the ground state and at finite temperatures. Both the Kondo- (well localized moments) and the mixed valence- (charge fluctuations) regimes are investigated. The effect of magnetic field and different electron fillings are considered. We find that: (i) The entanglement is governed by the hybridization, i.e. by the coupling between the conduction (c-) electrons and the local moments due to the f-electrons (see Fig. 1). At small hybridization the entanglement is predominantly nonlocal, between f-electrons, while at large hybridization it is local, between f- and c-electrons. The local f-entanglement survives at much higher temperatures than does the nonlocal -entanglement. (ii) These properties can be represented by an entanglement phase diagram, providing a view on the Kondo-RKKY competition complementary to the Doniach phase diagram. (iii)

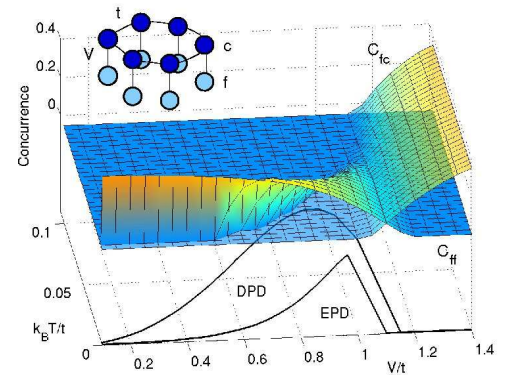


FIG. 1: The concurrences  $C^{(1)}$  and  $C_{fc}^{(0)}$  as a function of  $k_B T/t$  and  $V/t$  for  $L = 6$ ,  $U = 2E_f = 6t$ ,  $B = 0$  and half filling. Projected at the bottom is the Doniach, DPD, and the corresponding entanglement phase diagram, EPD (see text). The  $L = 6$  cluster is also shown.

In the mixed valence regime, at finite magnetic field and away from half filling we find nontrivial multiparticle entangled states. (iv) Charge dynamics plays an essential role in obtaining the results (i) to (iii). Our results illustrate the richness of entanglement properties of the PAM and invite to further investigations of additional regions in parameter space, disorder and geometry effects, etc.

Model and theory We study ring shaped clusters with  $L = 2$  to 6 sites and two orbitals per site, denoted  $c$  and  $f$  (see Fig. 1 for  $L = 6$ ). Each cluster has  $N_e$  electrons, with  $0 \leq N_e \leq 4L$ . The PAM cluster Hamiltonian is

$$H = \sum_i t \sum_{\langle ij \rangle} (c_i^\dagger c_j + h.c.) + U \sum_i n_i^f n_{i\#}^f + E_f \sum_i n_i^f + V \sum_i \sum_{\langle ij \rangle} (f_i^\dagger c_j + h.c.) + g \sum_B \sum_i S_i^z \quad (1)$$

with  $n_i^f = f_i^\dagger f_i$  and  $\langle ij \rangle = \langle i, j \rangle$ ,  $\# = c/f$ . Here  $hi; ji$  denotes nearest neighbor,  $n, n_{\#}$  sites and the spin operator  $\hat{S}_{ic} = (S_{ic}^x; S_{ic}^y; S_{ic}^z) = (1=2) \hat{\sigma}_{ic}^{\alpha}$ ,  $\hat{\sigma}_{ic}^{\alpha} = \sum_{\sigma} c_{i\sigma}^\dagger c_{i\sigma} \sigma_{\alpha}$  for  $c$  (similarly for  $f$ ), with  $\hat{\sigma}_{ic}^{\alpha} = (\sigma_x; \sigma_y; \sigma_z)$  a vector of Pauli matrices. The n.n. hopping between  $c$ -orbitals is  $t$  ( $t > 0$ ), whilst  $V$  is the hybridization term between  $c$  and  $f$ -orbitals at the same site: both  $t$  and  $V$  can be taken real. The orbital onsite interaction strength is  $U$ ,  $E_f$  is the energy of the  $f$ -orbitals and  $B$  is the magnitude of the uniform magnetic field.

We focus on the reduced two particle spin density matrix  $\rho^{(ij)}$ , for orbitals  $\sigma = f/c$  at sites  $i$  and  $j$ . Using the  $f^{\uparrow} |i\rangle; f^{\downarrow} |i\rangle; f^{\uparrow} |j\rangle; f^{\downarrow} |j\rangle$  basis, for e.g.  $\sigma = f$  the density matrix elements are  $h_{ij}^{\alpha\beta} = \langle f_i^\dagger f_j^\dagger \rho f_i f_j \rangle$  where  $h_{ij}^{\alpha\beta}$  denotes exact, many-body, thermal equilibrium averages. Due to translational invariance  $h_{ij}^{\alpha\beta}$  depends only on  $ji - jj$ . Since  $[\hat{H}; \sum_i S_i^z] = 0$ , each eigenstate has a well defined number of spin up and down electrons and only spin-conserving density matrix elements are nonzero. Consequently,  $\rho^{(ij)}$  has in general  $ve$  independent parameters:

$$\rho^{(ij)} = \begin{pmatrix} 0 & a & 0 & 0 & 1 \\ & a & 0 & 0 & 0 \\ & 0 & b & c & 0 \\ & 0 & c & b & 0 \\ & 0 & 0 & 0 & a \end{pmatrix} \quad (2)$$

Note that typically  $\text{tr}(\rho) \notin 1$ , since the number of electrons at each orbital can vary from zero to two. When  $B = 0$  spin symmetry requires [16] the state to be characterized by only two free parameters,  $c$  and  $a$ , with  $a = a$  and  $b = b = a - c$ : the state is a Werner state [17].

The entanglement is conveniently quantified via the concurrence [18]  $C(\rho) = C^{(ij)}(\rho) = \max\{0, \sqrt{\frac{1}{2}(\lambda_1 - \lambda_2 - \lambda_3 - \lambda_4)}\}$  where the  $\lambda_i$ s are the real and positive eigenvalues, in decreasing order, of the matrix  $\tilde{\rho}$ , where  $\tilde{\rho} = (\rho_{ij}^{\alpha\beta})_{\alpha\beta} = (\rho_{ij}^{\alpha\beta})_{\alpha\beta}$ . This gives [19] for  $\rho$  in Eq. (2)

$$C = 2 \max\{c - a, 0\} \quad (3)$$

We point out that in contrast to the single site Fock space, or mode entanglement considered e.g. in [13, 14], here the entanglement between two physical particles [20] is considered. The concurrence  $C$  in Eq. (3) is obtained from the reduced density matrix which by definition determines any two-particle observable, as e.g. correlation functions. Thus,  $C(\rho)$  is a natural measure for the experimentally accessible two particle entanglement.

Kondo-RKKY competition A central property of the PAM in the local moment (Kondo) regime is the competition between Kondo and RKKY correlations for the  $f$ -electrons. For macroscopic systems, such competition was described qualitatively by Doniach [5]: for low temperature  $T$  and weak hybridization,  $V/t < 1$ , the localized  $f$ -electron spins are RKKY-ordered. Increasing  $V/t$  there is a cross over to local Kondo screening. Such competition occurs also in nanoclusters, where it is controlled both by  $V/t$  and the conduction level spacing [21]. A description in terms of a cluster Doniach diagram is possible [22]: A transition criterion was established by comparing spin correlators. Recently, similar results have been presented for the 2D Kondo lattice model [23].

To investigate the entanglement in the Kondo-RKKY competition, we consider the symmetric case  $U = 2E_f$  (the ground state  $|j_{\sigma} i\rangle$  is a singlet [6]), with well localized  $f$ -electrons at half filling ( $N_e = 2L$ ),  $B = 0$  and  $T = 0$ . Under these conditions the PAM can be mapped [24] onto the Kondo lattice model (KLM) [6], characterized solely by  $J = 8V^2/(U t)$ . In the KLM both the  $c$  and  $f$ -density matrices are normalized and thus parameterized by a single parameter  $a$ . The concurrence is given by  $C = \max\{1 - 6a; 0\}$  and can be directly related to the spin correlator  $K^{(ij)} = \langle S_i^z S_j^z \rangle$  as  $C = \max\{1 - 2K; 0\}$ , where  $K = a^{-1} = 4$ .

Preliminary insight in the Kondo-RKKY competition is gained from the KLM in the simple case  $L = 2$ , where  $|j_{\sigma} i\rangle$  is obtained analytically. For the two limiting cases,

$$|j_{\sigma} i\rangle = \begin{cases} \frac{1}{\sqrt{8}} (f_1^\dagger f_2^\dagger - f_1^\dagger f_2^\dagger) (c_1^\dagger + c_2^\dagger) (c_1^\dagger + c_2^\dagger) |j_{\sigma} i\rangle & J \rightarrow 0 \\ (1=2) (f_1^\dagger c_1^\dagger - f_1^\dagger c_1^\dagger) (f_2^\dagger c_2^\dagger - f_2^\dagger c_2^\dagger) |j_{\sigma} i\rangle & J \rightarrow 1 \end{cases} \quad (4)$$

Thus, on increasing  $J$  from 0 (small hybridization), the system evolves from a maximally entangled, singlet state to a product state of  $cf$ -singlets (see Fig. 2). At  $J = 1/2$  we have  $C^{(1)} = C_{fc}^{(0)}$ . Qualitatively this is similar to what occurs in the two-in-purity Kondo [9] and Kondo necklace [10] models.

For  $L = 3$  (using numerical ED with  $U = 2E_f = 6t$ ), the physical picture for  $V < t$  is very different from the  $L = 2$  case: The properties of  $|j_{\sigma} i\rangle$  depend strongly on size effects such as even-odd  $L$  parity and the density and configuration of the  $c$ -electron levels. This is clearly illustrated by the drop of  $C^{(1)}$  from 1 for  $L = 2$  to 0 for  $L = 3$ , shown in Fig. 2. Interestingly, between  $L = 3$  and  $L = 6$ ,  $C^{(1)}$  increases monotonically with  $L$  from 0 to 0.4.

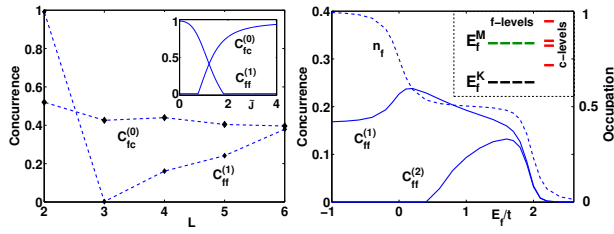


FIG. 2: Left: Concurrence  $C^{(1)}$  (for  $V = 0.2t$ ) and  $C^{(0)}$  (for  $V = 1.5t$ ) as a function of system size  $L$ . Inset:  $C^{(1)}$  and  $C^{(0)}$  as a function of  $J$  for the  $L = 2$  KLM. Right:  $C^{(1)}$  and  $C^{(2)}$  and the total  $f$ -level occupation  $n_f$  as a function of  $E_f/t$  in the mixed valence regime,  $V = 0.1t; U = 6t$  and  $L = 4$ . The energy level scheme for  $V = t$  is shown as inset:  $E_f^M$  ( $E_f^K$ ) denotes the  $f$ -level in the mixed valence (Kondo) regime.

This behavior follows from an increasing weight in  $j_{gi}$  of a superposition of a component with anti-ferromagnetic like order (not perfect for odd  $L$ )  $|j_{\uparrow\uparrow\uparrow}\dots\rangle$  and the same component with two neighboring spins flipped.

We also note that, for  $L = 4$  to  $6$ ,  $C^{(2)} = 0$  while for  $L = 6$  second next n.n. concurrence is again finite,  $C^{(3)} \approx 0.15$ . The nonlocal concurrences  $C_{fc}^{(j)}$ ;  $C_{cc}^{(j)}$  with  $j \geq 1$  are typically small or zero and will not be discussed further. It is important to note that  $j_{gi}$  always contains some doubly occupied  $c$ -orbitals, making the result qualitatively different from the Kondo necklace model [10]. Also, an effective RKKY spin Hamiltonian  $[6]_{i \neq j} J_{ij} \hat{S}_{i\uparrow} \hat{S}_{j\uparrow}$  gives a very different  $j_{gi}$ , and hence concurrence for most  $L$ . This provides strong evidence that the  $c$ -electron dynamics is essential for the obtained results. Both  $c$ - and  $fc$ -entanglement decrease monotonically on increasing the temperature  $T$ , since unentangled excited states get progressively populated. At  $k_B T \approx 0.1t$  (the typical energy scale of the low-lying spin excitations at  $V < t$ )  $c$ -entanglement is suppressed, whilst  $fc$ -entanglement persists to much higher  $T$ .

A global picture of the entanglement properties of the system is provided by an entanglement phase diagram, shown for  $L = 6$  in Fig. 1. The phase boundary shows the crossover temperature for which  $C = C_{fc}$ . Importantly, for  $V < t$  the entanglement and the Dombach phase diagram (also in Fig. 1) have distinctly different crossover temperatures. Increasing  $T$  from 0 the system thus passes three different phases: i) finite  $c$ -entanglement and dominating  $c$ -spin correlators  $\mathcal{K}^{(1)} |j\rangle > \mathcal{K}_{fc}^{(0)} |j\rangle$ ; ii) zero entanglement and  $\mathcal{K}^{(1)} |j\rangle > \mathcal{K}_{fc}^{(0)} |j\rangle$  and iii) zero entanglement and dominating  $fc$ -correlations  $\mathcal{K}_{fc}^{(0)} |j\rangle > \mathcal{K}^{(1)} |j\rangle$ . Moreover, there is a sharp cusp in the entanglement diagram due to the nonanalyticity of the concurrence at  $C = 0$ . This illustrates the importance of the entanglement phase diagram [25] as a new tool for analyzing the Kondo-RKKY competition.

Mixed valence regime. The effect of  $f$ -electron charge fluctuations on the entanglement manifests quite clearly when moving away from the Kondo regime. In the Kondo

limit the  $f$ -level energies are well below the conduction band,  $E_f \ll t; V$  and the occupation  $n_f = n_n^f + n_{\#}^f$  is essentially one, due to the large value of  $U$  ( $= 6t$ ) considered. However, when  $E_f$  enters the conduction band, the regime of mixed valence,  $n_f$  starts to decrease. We studied the mixed valence entanglement for  $1 < E_f/t < 3$ , i.e. with  $n_f \approx 1$  (deep below the conduction band,  $E_f + U < 2t$ , the  $f$ -levels are doubly occupied and inert).

We find that only for  $V < t$  there is additional entanglement away from the Kondo regime. In Fig. 2, we plot  $C$  as a function of  $E_f/t$  for  $L = 4$ . When  $n_f$  starts to drop, both n.n. and next n.n. entanglement increase, with a maximum at  $E_f = 0.2t$  and  $1.7t$ , respectively. This can be understood from the manybody wavefunction around  $E_f \approx t$ , where the  $f$ -level occupation is roughly  $1=2$ , i.e. on average two electrons occupy the  $f$ -levels. An analysis of the exact wavefunction shows that to a good approximation  $j_{gi}$  can be written as  $j_{gi} = j_{fi} - j_{ci}$ , with

$$j_{fi} = \frac{1}{12} \sum_{i \neq j} X_{if}^Y f_{j\#}^Y - \frac{1}{12} \sum_{i \neq j} Y_{i\#}^Y f_{j\#}^Y |j\rangle; \quad (5)$$

a linear combination of  $f$ -electron singlets. The  $j_{fi}$  in Eq. (5) gives a concurrence  $C^{(1)} = C^{(2)} = 1/6$ , in reasonable agreement with the ED results in Fig. 2. The value  $1/6$  comes entirely from the low occupation of the  $f$ -levels,  $\text{tr}(\rho) = 1/6$ , since the singlet itself is maximally entangled. As in the Kondo regime, the entanglement is suppressed at  $k_B T \approx 0.1t$ . The same result is found for all  $L$ , with the  $E_f/t$  interval of additional entanglement given by the density of states in the conduction band.

Finite B-eld Applying a magnetic field  $B$ , a naive expectation would be that aligning more and more spins along the direction of the field would progressively suppress the entanglement towards zero. It was however found in spin clusters [12] that at strong magnetic fields, with all spins but one flipped, the state is  $|j_{\uparrow\uparrow\uparrow}\dots\rangle + |j_{\#}\dots\rangle$ ; a strongly multiparticle entangled  $W$ -state [26]. This motivates an investigation the effect of  $B$  on the entanglement in the PAM.

We plot (see Fig. 3)  $C^{(1)}$  and  $C_{fc}^{(0)}$  as a function of  $B$  and  $V=t$  for  $L = 6$ . Since  $[\sum_i S_i^z; H] = 0$  a finite  $B$ -field only shifts all the manybody states in energy an amount proportional to their total  $S_z$  quantum number, eventually inducing a crossing of the  $B = 0$  levels and changing the ground state. This is clearly illustrated in Fig. 3. On increasing  $B$ , the total ground state spin  $S^{\text{tot}}$  increments monotonically in steps of one, i.e.  $B$  induces successive flipping of the spins. While for  $V > t$  the  $fc$ -entanglement is suppressed on increasing  $B$ , the  $c$ -entanglement survives for  $V < t$  up to  $S^{\text{tot}} = 2$ . Notably, for next and second next n.n. sites, entanglement actually increases with  $S^{\text{tot}}$  and at  $S^{\text{tot}} = 2$  we have  $C^{(j)} \approx 0.3$  for all  $j = 1; 2; 3$  (Fig. 3). The analysis of the exact wavefunction shows that the ground state for

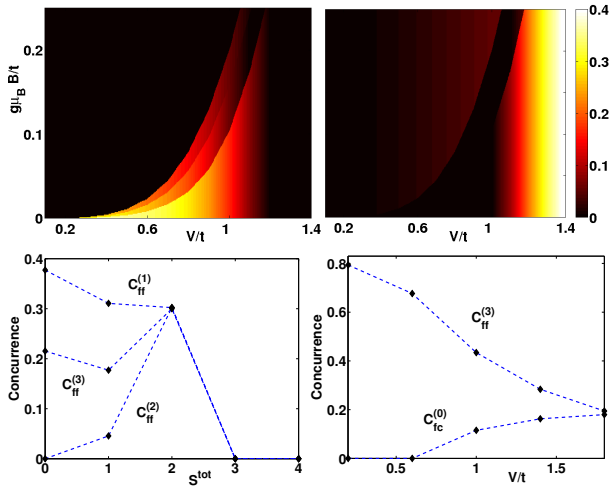


FIG. 3: Upper panels: The concurrence  $C^{(1)}$  (left) and  $C^{(0)}$  (right) as a function of magnetic field  $B$  and hybridization  $V=t$ . Lower left: The concurrence  $C^{(j)}$  for  $j = 1; 2; 3$  as a function of spin  $S^{\text{tot}}$ . Lower right: The concurrence  $C^{(1)}$  and  $C^{(0)}$  as a function of hybridization  $V=t$  for  $N_e = 8$  electrons. In all panels,  $L = 6$ ,  $E_f = U = 2 = 3t$  and  $T = 0$ .

$V = t$  is given by  $j_{gi} = j_{fi} - j_{ci}$ , with

$$j_{fi} = \sum_{i=1}^{X^6} f_{i\#}^Y f_{j\#}^Y j_i \quad (6)$$

This is a  $W$ -state, just as was found in spin clusters. A magnetic field thus flips the  $f$ -spins before flipping any  $c$ -spin, a consequence of the much higher cost (compared to  $0.01t$ ) in energy to flip a  $c$ -spin. In the  $W$ -state all particles are mutually entangled with the same axial pairwise concurrence  $C = 1/3$  [27], in good agreement with the ED results in Fig. 3. The  $W$ -state is found only for  $L = 6$ ; instead, for  $L = 3$  to  $5$  there is negligible entanglement away from  $S^{\text{tot}} = 0$ , an indication of a strong size dependence of this result.

Away from half filling. For  $N_e \notin 2L$ , the PAM phase diagram is rather complicated [6], in several parameter regimes the ground state is magnetic,  $S^{\text{tot}} > 0$ . To investigate the effect of the electron concentration on the entanglement, we considered fillings  $2L - 1 \leq N_e \leq L + 1$  for  $U = 2E_f = 6t$ ,  $B = 0$  and  $T = 0$ . We found that the overall behavior with  $f$ -entanglement at  $V < t$  and  $fc$ -entanglement at  $V > t$  prevails away from half filling. For  $V > t$ , reducing  $N_e$  monotonically suppresses the  $fc$ -entanglement, due to an incomplete local Kondo screening. Interestingly, for  $V < t$  we find finite  $f$ -entanglement only for  $L = 4; 6$  with  $N_e = L + 2$ . Since  $n_f = 1$ , this corresponds to two electrons in the conduction band. For this filling, the KLM ground state exhibits  $f$ -spin dimerization for  $L = 4$  and  $6$  respectively [28]. We indeed find that the many-body ground state is dominated by the term  $j_i = j_{fi} - j_{ci}$ , with  $j_{fi}$  a linear combi-

nation of  $L$  dimerized terms,

$$j_{fi} = 2^{-1} [j_{\#i} + j_{\#\#i} + j_{\#\#\#i} + j_{\#\#\#\#i}] \quad (7)$$

for  $L = 4$  and similar for  $L = 6$ . This state has the property that only sites opposite to each other in the ring show a finite entanglement,  $C^{(L=2)} = 4=L$ , in reasonable agreement with the numerical results (see Fig. 3).

In conclusion, we have studied two-body entanglement in Anderson nanoclusters. We presented an entanglement phase diagram describing a generic entanglement scenario for systems with Kondo-RKKY competition. We also showed that Anderson nanoclusters exhibit multipartite entanglement depending on parameter regimes, electron filling or applied magnetic fields. More generally, our results give evidence that the interplay of charge and spin degrees of freedom must be taken into account to assess the entanglement behavior of nanoclusters with magnetic impurities. We acknowledge useful discussions with C.-O. Anlauf. This work was supported by the Swedish VR (P.S.) and EU 6th framework Network of Excellence NANOQUANTA (NMP4-CT-2004-500198) (C.V.).

- 
- [1] M. Nielsen and I. Chuang, *Quantum Computation and Quantum Information*, (Cambridge University Press, Cambridge 2000).
  - [2] H.C. Manoharan, C.P. Lutz and D.M. Eigler, *Nature* 403, 512 (2000).
  - [3] T.W. Odom et al., *Science* 290, 1549 (2000).
  - [4] N.J. Craig et al., *Science* 301, 565 (2004).
  - [5] S. Doniach, *Physica B+C* 91, 231 (1977).
  - [6] H. Tsunetsugu, M. Sigrist and K. Ueda, *Rev. Mod. Phys.* 69 809 (1997).
  - [7] G.R. Stewart, *Rev. Mod. Phys.* 73, 797 (2001).
  - [8] S. Oh, J.Kim, *Phys. Rev. B* 73, 052407 (2006); E. S. Sørensen et al., *cond-mat/0606705*.
  - [9] S.Y. Cho, R.H. McKenzie, *Phys. Rev. A* 73, 012109 (2006).
  - [10] A. Saguia, M.S. Sarandy, *Phys. Rev. A* 67, 012315 (2003).
  - [11] K.M. O'Connor, W.K. Wootters, *Phys. Rev. A* 63, 052302 (2001); X. Wang, H. Fu, and A.I. Solomon, *J. Phys. A: Math. Gen.* 34 11307 (2001); I. Bose and A. Tribedi, *Phys. Rev. A* 72, 022314 (2005).
  - [12] M.C. Amesen, S. Bose, and V. Vedral, *Phys. Rev. Lett.* 87, 017901 (2001); G.L. Kamta and A.F. Starace, *ibid* 88, 107901 (2002).
  - [13] S.-J. Gu, et al., *Phys. Rev. Lett* 93, 086402 (2004).
  - [14] D. Larsson, H. Johannesson, *Phys. Rev. Lett* 95, 196406 (2005); *Phys. Rev. A* 73, 042320 (2006).
  - [15] A. Osterloh et al., *Nature* 416, 608 (2002); T.J. Osborne and M.A. Nielsen, *Phys. Rev. A* 66, 032110 (2002).
  - [16] P. Nozières, *Theory of Interacting Fermi Systems*, (Benjamin, N.Y. 1964).
  - [17] R.F. Werner, *Phys. Rev. A* 40, 4277 (1989).
  - [18] W.K. Wootters, *Phys. Rev. Lett* 80, 2245 (1998).
  - [19] Since states with zero or two particles at an orbital do not contribute to the entanglement, we have  $0 \leq C \leq 1$ .

- [20] H. M. Wiseman, J.A. Vaccaro, Phys. Rev. Lett. 91, 097902 (2003).
- [21] C. Verdozzi, Y. Luo, N. Kibussis, Phys.Rev. B 70, 132404 (2004).
- [22] Y. Luo, C. Verdozzi, N. Kibussis, Phys. Rev. B 71, 033304 (2005).
- [23] I. Zarec, B. Schmidt and P. Thalmeyer, Phys.Rev.B 73, 245108 (2006).
- [24] J.R. Schrieffer, P.A. Wolf, Phys.Rev. 149, 491 (1966).
- [25] Changing  $t$ , i.e. the conduction energy level spacing, the entanglement phase diagram is scaled in size.
- [26] W. Dur, G. Vidal, J.I. Cirac, Phys. Rev. A 62, 062314 (2000); X. Wang, *ibid* 64, 012313 (2000).
- [27] V. Cooman, J. Kundu and W. K. Wootters, Phys. Rev. A 61, 052306 (2000).
- [28] J.C. Xavier et al, Phys.Rev.Lett. 90, 247204 (2003), Y. Chen and H. Chen, Phys.Rev.B 73, 033402 (2006).